Investigation of Ground- and Excited-State Photophysical Properties of 5,10,15,20-Tetra(4-pyridyl)-21H,23H-porphyrin with Ruthenium Outlying Complexes

ARTICLE *in* THE JOURNAL OF PHYSICAL CHEMISTRY A · DECEMBER 2011

Impact Factor: 2.69 · DOI: 10.1021/jp205963k · Source: PubMed

13 AUTHORS, INCLUDING:

Antonio Eduardo Da Hora Machado
Universidade Federal de Uberlândia (UFU)
116 PUBLICATIONS **1,152** CITATIONS
SEE PROFILE

Alexandre Marletta
Universidade Federal de Uberlândia (UFU)
100 PUBLICATIONS **504** CITATIONS
SEE PROFILE

Alzir Batista
Universidade Federal de São Carlos
169 PUBLICATIONS **2,042** CITATIONS
SEE PROFILE

Newton M Barbosa Neto
Universidade Federal de Uberlândia (UFU)
51 PUBLICATIONS **454** CITATIONS
SEE PROFILE

THE JOURNAL OF PHYSICAL CHEMISTRY A

ARTICLE

pubs.acs.org/JPCA

Investigation of Ground- and Excited-State Photophysical Properties of 5,10,15,20-Tetra(4-pyridyl)-21H,23H-porphyrin with Ruthenium Outlying Complexes

R. N. Sampaio,[*,†] W. R. Gomes,[‡] D. M. S. Araujo,[‡] A. E. H. Machado,[‡,§] R. A. Silva,[†] A. Marletta,[†] I. E. Borissevitch,[∥] A. S. Ito,[∥] L. R. Dinelli,[⊥] A. A. Batista,[#] S. C. Zílio,[▽] P. J. Gonçalves,[○] and N. M. Barbosa Neto[†]

[†]Instituto de Física, Universidade Federal de Uberlândia, Minas Gerais, Brazil

[‡]Instituto de Química, Universidade Federal de Uberlândia, Minas Gerais, Brazil

[§]Departamento de Química, CAC/UFG, Campus Catalão, Universidade Federal de Goiás, Goiás, Brazil

[∥]Faculdade de Filosofia Ciências e Letras de Ribeirão Preto, Universidade de São Paulo, São Paulo, Brazil

[⊥]Faculdade de Ciências Integradas do Pontal, Universidade Federal de Uberlândia, Minas Gerais, Brazil

[#]Departamento de Química, Universidade Federal de São Carlos, São Paulo, Brazil

[▽]Instituto de Física de São Carlos, Universidade de São Paulo, São Paulo, Brazil

[○]Instituto de Física, Universidade Federal de Goiás, Goiás, Brazil

ABSTRACT: The present work employs a set of complementary techniques to investigate the influence of outlying Ru(II) groups on the ground- and excited-state photophysical properties of free-base tetrapyridyl porphyrin (H_2TPyP). Single pulse and pulse train Z-scan techniques used in association with laser flash photolysis, absorbance and fluorescence spectroscopy, and fluorescence decay measurements, allowed us to conclude that the presence of outlying Ru(II) groups causes significant changes on both electronic structure and vibrational properties of porphyrin. Such modifications take place mainly due to the activation of nonradiative decay channels responsible for the emission quenching, as well as by favoring some vibrational modes in the light absorption process. It is also observed that, differently from what happens when the Ru(II) is placed at the center of the macrocycle, the peripheral groups cause an increase of the intersystem crossing processes, probably due to the structural distortion of the ring that implies a worse spin−orbit coupling, responsible for the intersystem crossing mechanism.

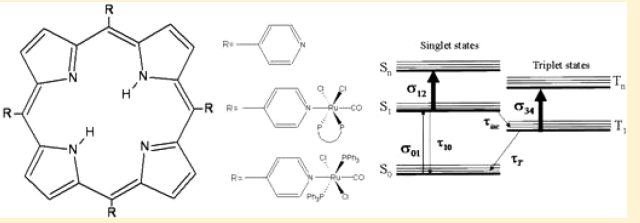

1. INTRODUCTION

Porphyrins are aromatic macrocyclic molecules formed by four pyrrole rings linked by unsaturated methylene bridges.[1] This class of compounds is present in a great variety of natural processes such as photosynthesis (Mg porphyrins), oxygen transport and storage (iron porphyrins), and in many others.[2] Besides the interest in understanding these natural processes, porphyrins are also widely studied because of their potential applications in fields such as photonics,[3] medicine (e.g., cancer therapy),[4,5] gas sensors,[6] molecular devices,[7,8] energy conversion, and solar cells.[9] In free-base types, two central protons are linked to the nitrogen atoms of the porphyrin ring to assure structural stability.[1] In particular, 5,10,15,20-tetra(pyridyl)-21H,23H-porphyrin is formed by four pyridyl groups attached to the mesocarbons of the macrocycle, as shown in Figure 1.

A major advantage of this class of compounds is the possibility of carrying out structural modifications that can tune some specific property with the aim of improving its behavior. Efforts in this direction have been made through changes of the central ion,[10,11] aggregate formation,[12] insertion of lateral and axial ligands,[13−15] oligomers,[16] isomeric structures,[17] cationic porphyrins,[18] and others. Systematic studies on the relation between photophysical properties and molecular structure are necessary to understand these modifications.

Due to the electronic similarity between ruthenium and iron, the role of ruthenium placed at the center of the macrocycle and the influence of different types of ligands on the photophysical and photochemical properties of porphyrins has been exhaustively investigated in the past decades.[19−23] It is known that when Ru^{2+} is inserted at the center of the macrocycle, the resulting irregular porphyrin gives rise to a strong suppression of the emission due to the intense interaction between the central ion and the π electrons of the macrocycle ring.[1,19] Moreover, a strong dependence between the nature of the axial ligand and the photophysical characteristics, mainly for the lowest excited-state, is also observed.[20] Concerning ruthenium outlying groups, great interest arises owing to its potential to form supramolecular porphyrins strucures,[24] which have great influence on the photophysical

Received: June 24, 2011
Revised: December 13, 2011
Published: December 14, 2011

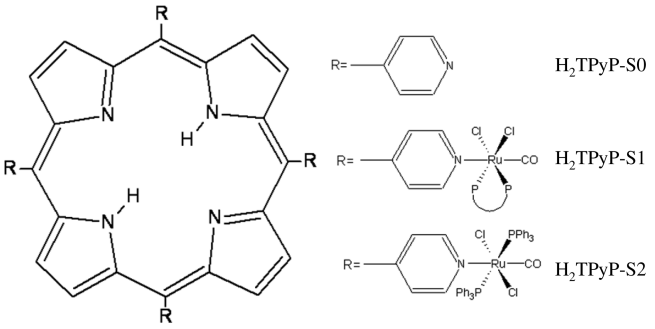

Figure 1. Molecular structure of the free base 5,10,15,20-tetra-(pyridyl)-21H,23H-porphyrin. R represents the peripheral groups linked to the macrocycle ring: Group 0 = pyridine (sample H_2TPyP-S0); Group 1 = pyridine + $RuCl_2$COdppb (sample H_2TPyP-S1); Group 2 = pyridine + $RuCl_2(CO)(PPh_3)_2$ (sample H_2TPyP-S2). dppb stands for P—P = bis-(diphenylphosphine)butane, and PPh_3 stands for triphenylphosphine.

properties of porphyrins.[15,24−26] In the present work, we study a regular type[1] of porphyrin having ruthenium groups interacting with the electrons of the porphyrin ring via a pyridine bridge, as depicted in Figure 1. Two different types of ligands were attached to Ru(II) and linked to porphyrin at peripheral positions. They are $[RuCl_2COdppb]$ and $[RuCl_2(CO)(PPh_3)_2]$ which, when linked to free-base tetrapyridyl porphyrin, form the complexes dubbed as H_2TPyP-S1 and H_2TPyP-S2, respectively. In the structure of ruthenium ligands, dppd (also represented by P—P in Figure 1) stands for bis(diphenylphosphine)butane, while PPh_3 stands for triphenylphospine.

2. MATERIALS AND METHODS

Samples. H_2TPyP was synthesized according to the procedure described in ref 27. The Ru^{2+} porphyrin complexes were synthesized under argon by reaction of H_2TPyP with $[Ru_2Cl_4(CO)_2(dppb)_3]$ and $[RuCl_2(CO)(DMF)(PPh_3)_2]$ to provide H_2TPyP-S1, and H_2TPyP-S2, respectively. The solutions were stirred for 4 h, and their volume was subsequently reduced by approximately 90%. The solutions were then filtered, and the filter cake was washed thoroughly with ethyl ether. Later, the powder obtained was dried in vacuum to give the desired compound. In this way, we synthesized $[H_2TPyP\{RuCl_2(CO)(PPh_3)_2\}_4]$, using 20 mg ($3.23 \times 10^{-5}$ mol) of H_2TPyP with 95 mg (1.29×10^{-4} mol) of $[RuCl_2(CO)(PPh_3)_2(DMF)]$ in 20 mL of dichloromethane. Yield: 64% (70 mg); Exp. (Calc.), %C = 62.68 (63.71); %H = 4.33 (4.24); %N = 3.72 (3.23); ν(CO), 1957 cm-1; 31P{1H}, δ 30.4, singlet, in CH_2Cl_2 as solvent. $[H_2TPyP\{RuCl_2(CO)(dppb)\}_4]$ was synthesized using 20 mg (3.23×10^{-5} mol) of H_2TPyP and 119.5 mg (6.7×10^{-5} mol) of $[Ru_2Cl_4(CO)_2(dppb)_3]$. Yield: 65% (65 mg); Exp. (Calc), %C = 59.74 (59.93); %H = 4.55 (4.51);

Spectroscopic Measurements. UV—visible (UV—vis) absorption spectra were obtained with a UV 1650 PC Shimadzu spectrophotometer, with the samples dissolved in chloroform and placed in a 1 cm-thick quartz cell. The fluorescence spectra were obtained by exciting the solutions with an argon ion laser at 514.5 nm and detecting the signal in a 90° configuration, with an USB 2000 Ocean Optics spectrophotometer. The concentrations employed in these optical measurements were always smaller than 1 μM (10^{16} molecules/cm^3). In particular, the fluorescence spectra were acquired in highly diluted solutions ($\ll$ 0.1 μM) in order to circumvent the inner filter effect.[28]

Fluorescence decay times were obtained with an apparatus based on the time-correlated single photon counting method. The excitation source was a titanium—sapphire laser (Tsunami 3950—Spectra Physics), pumped by the second harmonic of a diode-pumped Nd:YVO_4 laser (Millenia—Spectra Physics), and frequency doubled to 465 nm in a LBO crystal (GWN-23PL — Spectra Physics).

In order to investigate the excited-state photophysical parameters, we employed the well-known open aperture Z-scan technique,[29] which is based on the measurement of the sample transmittance as it translates through the focal plane of a Gaussian beam. Although the technique has been fully described elsewhere,[29−32] a few details of our experimental setup are presented here. As the excitation source, we used a frequency doubled, *Q*-switched, and mode-locked Nd:YAG laser, producing *Q*-switch envelopes with approximately 25 pulses separated by 13 ns, each of them with a duration of 70 ps. To determine the contributions of different excited-states, the samples were excited with either the complete pulse train or with a single pulse extracted from the *Q*-switch envelope by means of a Pockels cell. The use of a single pulse favors the observation of contributions coming from the first excited singlet state (S_1) before the triplet population builds up. On the other hand, the use of the complete set of pulses under the *Q*-switch envelope allows one to investigate accumulative nonlinearities related to the intersystem crossing, in a technique named pulse train Z-scan (PTZ-scan).[31] The amplitude of each peak detected is proportional to the pulse fluence because the detection system has a response time much longer than 70 ps pulse duration. The normalization of each pulse of the pulse train to that achieved when the sample is far from the focus produces a set of Z-scan signatures. They can be used to map the absorptive nonlinearity along the *Q*-switch envelope and to determine fast (subnanosecond) and cumulative contributions for the excited-state absorption. In all Z-scan experiments, the beam is focused to a diameter of about 40 μm with an f = 12 cm lens, and the samples were placed in a 2 mm-thick quartz cell to ensure that the thin sample approximation is applicable. The experimental data reported here were based on the average of three independent experiments.

The triplet state lifetime was monitored with the laser flash photolysis technique performed in a standard 1 cm-thick quartz cell. The excited-states were produced by 3 ns light pulses resulting from the second harmonic (532 nm) of a Nd:YAG laser. The decay profiles of the triplet state absorption were monitored at 476 nm, using a standard detection system. To diminish the triplet quenching by molecular oxygen, the samples were usually deoxygenated by bubbling nitrogen through the solution for 15 min.

3. RESULTS AND DISCUSSION

3.1. Absorbance Spectrum. The porphyrin UV—vis absorption spectrum shows two well-characterized bands: the Soret or B band and the Q-band. The Soret band is stronger and is generally located between 380 and 450 nm. This band is attributed to the transition to the second excited singlet state, being related to a strongly allowed electronic transition between the π and π^* orbitals of the porphyrin ring.[1] The Q-band is typically found between 500 and 650 nm and is related to the transition to the first excited singlet state. It is known[1] that the number of Q subbands depends on the symmetry of the molecule. In our case, the free-base porphyrin with two protons at the center of the

dx.doi.org/10.1021/jp205963k |*J. Phys. Chem. A* 2012, 116, 18–26

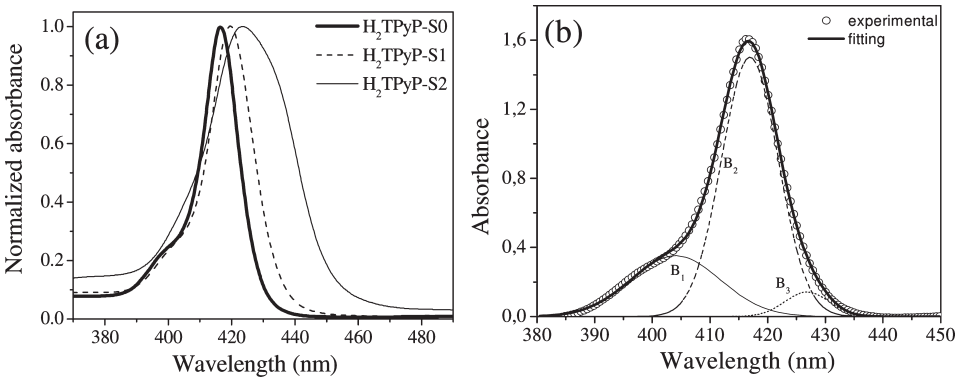

Figure 2. (a) Soret band for studied compounds and (b) deconvolution performed for H_2TPyP-S0.

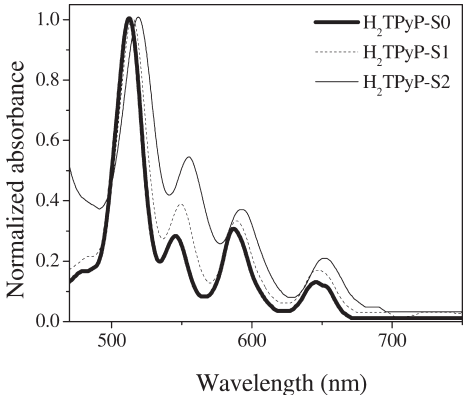

Figure 3. Q band for free-base tetrapyridyl porphyrins with and without outlying ruthenium groups.

macrocycle has D_{2h} symmetry and presents four well-defined Q sub-bands, namely $Q_x(0,0)$, $Q_y(0,0)$, $Q_x(1,0)$, and $Q_y(1,0)$.

Figure 2 shows the characteristic Soret band of the porphyrin complexes under study. The introduction of outlying groups causes a small red shift and a broadening of the band, especially when the $[RuCl_2(CO)(PPh_3)_2]$ group is present (sample H_2TPyP-S2). The red shift is observed for all porphyrin structures and implies that, differently from what happens in porphyrins with Ru(II) groups placed at the center of the ring, the π-backbonding originated from the CO ligand exerts low influence on absorption features.[19,20] The possibility of aggregation was not taken into account because no modifications were observed in spectra acquired at different concentrations. Furthermore, the very small concentrations used do not favor this effect in free-base tetrapyridyl porphyrins.[33]

A Gaussian deconvolution performed on the Soret band shows the presence of three overlapping sub-bands. The first is responsible for the shoulder observed around 400 nm (B_1), the second is the main peak located around 417 nm (B_2), while the third sub-band is located around 423 nm (B_3) (see Figure 2b). The B_3 sub-band is more sensitive to the addition of outlying ruthenium groups, especially when the PPh_3 ligand is present. This fact implies that the presence of a particular ligand enhances the contribution coming from this particular vibrational mode, and the red shift observed in the B-band can probably be attributed to the increase of the contribution assigned to B_3 sub-band.

Figure 3 presents the Q bands of the porphyrins investigated in this work. It is clear that they show a regular-type behavior that assures that D_{2h} symmetry remains, differently from what happens when ruthenium is inserted at the center of the macrocycle.[21] The only modification noted is the small red shift observed in the case of H_2TPyP-S2, and a change in the relative intensities of the Q sub-bands. The insertion of ruthenium outlying groups changes the Q bands intensity profile from *phyllo* to *etio* type. According to ref 34, Ru(II) compounds have an intense absorption band around 540 nm, assigned to a charge-transfer process. Therefore, the enhancement of the $Q_y(0,0)$ band intensity can be attributed to contributions coming directly from the absorption of the outlying groups.

In order to quantitatively confirm the influence of lateral groups on the absorption of Q-band, we followed Spellane et al.[35] and calculated the absorbance ratio Q(0,0)/Q(1,0) according to

$$\frac{Q(0,0)}{Q(1,0)} = \left[\frac{Q_x(0,0) + Q_y(0,0)}{Q_x(1,0) + Q_y(1,0)}\right] \quad (1)$$

which provides the relative intensity between the bands associated with 0⟶0 to 0⟶1 transitions.

Equation 2 below can be used to provide the oscillator strength of the absorption[36,37] associated with the Soret band and thus estimate the influence of the peripheral groups on the absorbance capacity of the H_2TPyP at the B band region.

$$f = \frac{4.32\times10^{-9}}{n}\int \varepsilon(k)\, dk \quad (2)$$

According to this equation, f is proportional to the integral of the molar absorption coefficient (ε) spectrum acquired at different wavenumbers (k, in cm^{-1}). ε is easily obtained from the absorbance spectrum considering that $A - \varepsilon Lc$,[37] where A is the absorbance of the solution measured, L is the optical path length of the quartz cell, and c is the molar concentration.

Table 1 summarizes the general features of the Soret and Q bands for H_2TPyP without and with different ruthenium outlying groups, while Table 2 summarizes the spectroscopic features of the three Soret sub-bands obtained from the fittings. The oscillator strengths for the Soret band were obtained by applying eq 2 directly to the experimental absorbance curves, while the oscillator strengths associated with Soret sub-bands were obtained with eq 2 applyed to the individual Gaussian curves found from the theoretical fitting of the measured absorbance.

From the data summarized in Tables 1 and 2, we verify that the insertion of outlying ruthenium groups magnifies the absorbance

dx.doi.org/10.1021/jp205963k |*J. Phys. Chem. A* 2012, 116, 18–26

Table 1. B- and Q-Band Absorption Features[a]

	B-band		Q-band				
porphyrin	f (× 10−3)	λ_c (nm)	$Q_y(1,0)$ $\lambda_{máx}$(nm)	$Q_y(0,0)$ $\lambda_{máx}$(nm)	$Q_x(1,0)$ $\lambda_{máx}$(nm)	$Q_x(1,0)$ $\lambda_{máx}$(nm)	[Q(0,0)]/[Q(1,0]
H_2TPyP-S0	13.77	416	513(1)	545(0.28)	588(0.31)	645(0.13)	0.31
H_2TPyP-S1	14.78	419	515(1)	549(0.39)	589(0.33)	647(0.17)	0.42
H_2TPyP-S2	18.86	423	519(1)	555(0.54)	592(0.37)	650(0.21)	0.55

[a] f stands for oscillator strength, λ_c is the band center position. The values in parentheses are the relative intensities of the Q band in relation with $Q_y(1,0)$.

Table 2. The Soret Sub-bands Spectroscopic Features[a]

	Sub-Band B1			Sub-Band B2			Sub-Band B3		
porphyrin	f (× 10^{-3})	λ_c (nm)	Γ (nm)	f (× 10^{-3})	λ_c (nm)	Γ (nm)	f (× 10^{-3})	λ_c (nm)	Γ (nm)
H_2TPyP-S0	3.32	404	18.21	5.66	417	11.6	0.48	427	9.1
H_2TPyP-S1	2.38	405	17.1	2.76	419	13.3	5.04	428	13.7
H_2TPyP-S2	1.79	410	20.4	3.88	420	12.1	5.47	430	23.2

[a] f is the oscillator strength, λ_c is the band center position, and Γ is the full width at half maximum (fwhm).

of the Soret band, especially of the B_3 sub-band. Such enhancement occurs due to both the broadening as well as the red shift suffered by the Soret band. On the other hand, comparing the tetraruthenated samples with H_2TPyP-S0, we see that the insertion of outlying groups is always deleterious to the absorption of the sub-bands B_1 and B_2.

Concerning to the Q-band, we note that ruthenium groups substantially increase the absorbance ratio (Q[0,0]/Q[1,0]), meaning that the 0→0 transition is favored. As expected from the result for the B band, the major modification is again caused by the $[RuCl_2(CO)(PPh_3)_2]$ group. Finally, it is important to emphasize that the spectroscopic features presented by the absorbance bands of the samples investigated are quite similar to other tetrapyridyl supramolecular structures.[15,25,26,38]

3.2. Fluorescence Spectrum. Generally, porphyrins present two fluorescence bands located around 650 and 700 nm, and then it is characterized by a significant red emission. In particular, H_2TPyP presents two peaks centered at 647 nm (the stronger one) and 709 nm.[27] Figure 4 shows the fluorescence spectra for H_2TPyP without and with the ruthenium outlying groups.

The presence of ruthenium groups with $[RuCl_2(CO)(PPh_3)_2]$ (sample H_2TPyP-S2) causes small red shifts in the fluorescence, similar to other tetraruthenated porphyrins,[25] being assigned to the decrease in the highest occupied molecular orbital to lowest unoccupied molecular orbital (HOMO−LUMO) gap observed from the absorbance spectra (Q-band red shift). No shift is observed for H_2TPyP-S1. The fluorescence spectra features are listed in Table 3.

Aiming to investigate the presence of possible quenching processes, we estimated the fluorescence quantum yield and verified the influence of the ruthenium groups on the radiative decay efficiency of the H_2TPyP. For calibration, we used an aqueous solution of rhodamine B as a reference[39] because it presents two good features: (1) it has emission located at nearly the same spectral region as that of the porphyrins and (2) it has a good fluorescence quantum yield ($\Phi_{rhodamine} \cong$ 0.31 in water solution[39]), which assures an easily detectable fluorescence signal. Φ_{fl} was determined by comparing it with the standard, and calculated according to the following

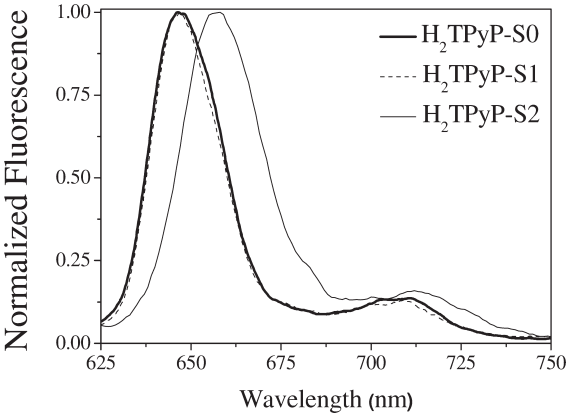

Figure 4. Fluorescence spectra, at room temperature, for free-base tetrapyridyl porphyrins dissolved in chloroform with and without outlying ruthenium groups. λ_{exc} = 514 nm.

equation:[36,39]

$$\Phi_{fl} = \Phi_{fl0}\frac{F_{fl}}{F_{fl0}}\frac{A_0}{A}\frac{n^2}{n_0^2} \quad (3)$$

where Φ_{fl} and Φ_{fl0} are the quantum yields of the compound investigated and of the reference, respectively. F_{fl} and F_{fl0} are the integrated fluorescence intensities of the compound and reference samples, and A and A_0 are the absorbances at the excitation wavelength of the compound and reference solutions. n's are the refractive indexes of solvent containing the compound (n) and the reference (n_0).

All experiments were performed in the presence of oxygen at a very low solute concentration, and the fluorescence quantum yield values obtained are presented in the Table 3. One can observe that the inclusion of ruthenated peripheral groups causes a fluorescence quenching, indicating the activation of nonradiative decay paths. Such quenching is always observed when ruthenium peripheral groups are present, increasing with the number of adducts in the supramolecular structure.[25]

dx.doi.org/10.1021/jp205963k |J. Phys. Chem. A 2012, 116, 18–26

Table 3. Fluorescence Features for Porphyrin[a]

sample	Q(0,0) λ_c(nm)	Q(1,0) λ_c(nm)	Φ ($\times 10^{-3}$)	τ_1 (ns)	τ_2 (ns)	τ_3 (ns)
H_2TPyP-S0	647	706	17	8	0	0
H_2TPyP-S1	647	708	9	4.7	0	0
H_2TPyP-S2	657	713	1	4.6(2.6 $\times 10^3$)	1.6(5.7 $\times 10^4$)	0.6(2.8 $\times 10^7$)

[a] λ_c is the band center position, Φ is the fluorescence quantum yield, and τ_i ∴ i = 1,2,3 are the decay times. The values inside the brackets are the amplitudes of the decays.

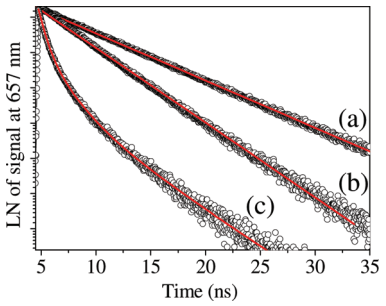

Figure 5. Fluorescence decay curves for (a) H_2TPyP-S0, (b) H_2TPyP-S1, and (c) H_2TPyP-S2. The open black circles are the experimental points, and the solid red lines are the theoretical exponential fittings. The samples were excited at 470 nm, and the emission was collected at 657 nm.

In order to obtain more information about possible new deactivation paths, we carried out fluorescence decay measurements, as described in Section 2. Figure 5 presents fluorescence decay profiles obtained for the samples investigated, while the decay times are shown in Table 3. The porphyrin without outlying ruthenium groups presents a monoexponential decay time of 8 ns attributed to the depopulation of the first singlet excited state (Q-band) by two possible paths: $S_1 \rightarrow S_0$ relaxation and intersystem crossing conversion.[27] For molecules with ruthenium outlying groups, fluorescence decay times are always reduced, and for sample H_2TPyP-S2, two new faster decay times were detected. The decrease of the fluorescence time and the appearance of new decays strongly support the hypotheses of the activation of a nonradiative path due to the insertion of ruthenium groups in the H_2TPyP structure. It is important to note that, besides the two extra decay times, H_2TPyP-S2 also presents low quantum yields.

The possible mechanisms responsible for the quenching are as follows: (i) *Energy transfer*: Such mechanism takes place from the excited donor moiety (in our case, the excited porphyrin ring), generating an excited acceptor unit (ruthenium group), in a process well described in ref 24. As it is known, ruthenium moieties do not decay radiatively,[25,34] which implies that the quenching process can be caused by the energy transfer from the porphyrin ring to the ruthenium group via the pyridyl bridge, with the subsequent nonradiative dissipation of such energy by the outlying units. Such process implies just the quenching of the porphyrin emission, with no modification of the fluorescence shape, exactly as measured in our experiments and in other similar samples.[15,25] (ii) *Aggregate formation*: As mentioned before, the aggregate formation is disregarded because no changes occurred in the absorbance and fluorescence spectral shape obtained in solutions with different porphyrin concentrations. This fact strongly suggests that no aggregation takes place for the samples employed in this investigation. (iii) *Creation of new vibrational modes*: Such possibility is corroborated by the fact that the insertion of the outlying groups implies an increase of the Soret-bandwidth, which can be explained as being due to the creation of new vibrational modes. The presence of ruthenium groups creates a more complex supramolecular structure with more degrees of freedom and, consequently, more possible vibrational modes. These new modes could dissipate energy in a nonradiative way. (iv) *Electron transfer*: It is known that in such structures a metal-to-ligand electron transfer from ruthenium to porphyrin ring can occur and can be responsible for the quenching of the fluorescence.[1] However Prodi et al.[25] investigated similar tetrapyridyl porphyrin structures and observed no correlation between electron-transfer energy, obtained from electrochemical measurements, and quenching efficiency.

Table 3 also shows that for H_2TPyP-S2, the shorter decay time (0.6 ns) presents the highest amplitude, which indicates its predominance as a decay channel. This observed subnanosecond decay component could be explained by considering the structural conversion of the porphyrin in different structural isomers. According to ref 17, such H_2TPyP supramolecular structures can present two isomeric forms. As described in other systems,[40] the conversion between the two possible isomeric structures can be photoinduced in a process that involves the following steps: (1) The molecule is promoted to an electronic excited-state via one-photon absorption and (2) from this higher energetic level, the molecule has enough energy to overcome the potential barrier that separates the two isomeric structures. So, in the relaxation process, the molecule can be converted to another isomeric structure. Generally, such relaxation via isomeric change occurs at a subnanosecond time scale.[41]

Finally, an additional strong quenching mechanism present in such systems is the intersystem crossing, responsible for the activation of spin-forbidden transitions.[25,36,42] Particularly, for the supramolecular structures investigated, two intersystem crossing processes are available: (i) the usual intersystem crossing within the porphyrin ring[1,27] and (ii) the intersystem crossing from the excited singlet state of the porphyrin ring to the excited triplet state of the ruthenium moiety.[15,25] Aiming to investigate the influence of singlet−triplet conversion on the decay paths of our porphyrin samples, we performed a complete set of excited-state dynamics meausrements presented in the next section.

3.3. Excited-State Dynamics. The results presented up to now provided information about the ground-state absorption and the first singlet excited state decay, besides pointing to the necessity of understanding the real importance of the intersystem crossing mechanism to the quenching process. Moreover, we have recently observed that tetraruthenated porphyrins present sequential two-photon absorption at the nanosecond regime,[14] but no information about the excited-state absorption dynamics was obtained until now. In order to accomplish this task, we performed Z-scan measurements with single 70 ps pulses and with pulse trains (PTZ-scan), in association with laser flash

dx.doi.org/10.1021/jp205963k |J. Phys. Chem. A 2012, 116, 18–26

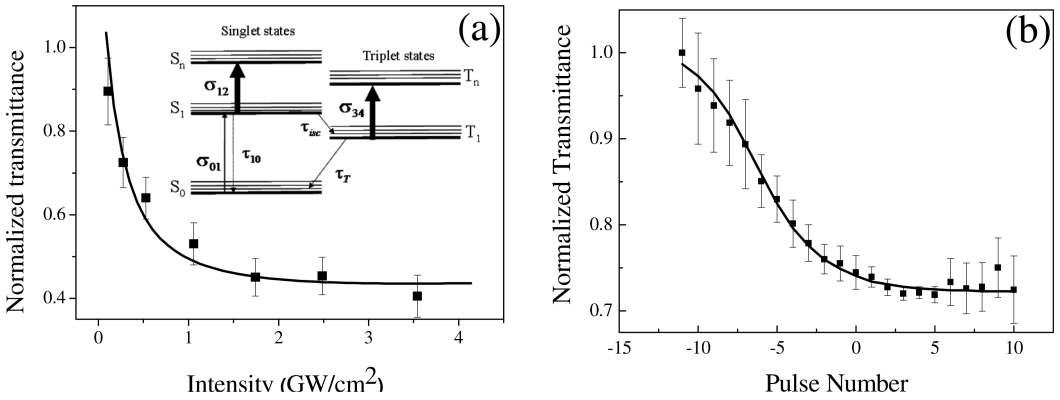

Figure 6. (a) Normalized transmittance versus 70 ps pulse intensity and (b) typical Z-scan pulse train signal, both obtained for H_2TPyP-S1. Solid squares are experimental. Points and solid lines are theoretical fittings obtained solving the correspondent set of rate equations. The inset in panel a corresponds to the Jablonski diagram.

photolysis experiments. The results obtained with these techniques, together with the absorbance spectrum and fluorescence decay measurements, enabled us to fully determine the parameters associated with the Jablonski diagram. This diagram is a five-energy-level diagram that describes all processes caused by the incidence of resonant radiation on the porphyrin;[1,42] see inset of Figure 6a. The diagram includes the ground-state singlet level (S_0), two excited singlet levels (S_1 and S_n), and two excited triplet levels (T_1 and T_n). Under resonant conditions, one-photon absorption largely exceeds simultaneous two-photon absorption (2PA) from the ground-state. Thus, we neglected any 2PA contribution and assumed that nonlinear absorption is only produced by two sequential one-photon absorptions from the ground- and excited-states.[32] It is also assumed that, at room temperature, the molecules occupy the lowest vibronic level of the lowest electronic state S_0. In addition, the contribution caused by the intersystem crossing from the porphyrin ring to the ruthenium moiety is not considered in our energy level model, since just one single $T_1 \rightarrow S_0$ decay time is observed, for all samples investigated. Such observation is corroborated for similar systems in ref 25.

Exciting the solutions with 532 nm laser pulses promotes molecules to a vibronic level of S_1 via a one-photon process, with a ground-state absorption cross-section σ_{01}. The molecules excited to higher vibronic levels of S_1 first relax to lower vibronic levels and then undergo one of the following three processes: (i) decay to S_0 with the time constant τ_{10}, (ii) suffer an intersystem crossing to the porphyrin triplet state T_1, with the time constant τ_{isc}, or (iii) are promoted, by one-photon absorption, to a vibronic level of a higher excited state, S_n, with an absorption cross-section σ_{12}. The population created in the triplet state can also suffer one-photon excitation to a vibronic level of the higher excited triplet state T_n, with an absorption cross-section σ_{34} or relax to the ground state S_0, with the triplet lifetime τ_T. However, as τ_T is much longer than the pulse train duration employed in the experiment (see Table 4), the contribution of such relaxation (n_{T_1}/τ_T) is negligible and does not contribute to the decrease of the triplet state population during the interaction of the molecules with the pulse train. Moreover, the population of higher vibronic excited-states occurring during excitation can be neglected, since their lifetime is much shorter than the excitation pulse duration. We also assumed that the lifetime of the highest electronic excited-states is on the order of hundreds of femtoseconds.[10,21] With these considerations, the complete set of rate equations that describes the excited-state dynamics involving the singlet and triplet states are[10,27,32,43,44]

Table 4. Excited-State Dynamics Parameters[a]

sample	$\sigma_{01} \times 10^{-17b}$ (cm^2)	$\sigma_{12} \times 10^{-17b}$ (cm^2)	$\sigma_{34} \times 10^{-17b}$ (cm^2)	τ_{isc} (ns)	τ_T (μs)
H_2TPyP-S0	1.6[c]	4.0[c]	2.1[c]	14[c]	1.4
H_2TPyP-S1	3.0	4.5	3.4	19	120
H_2TPyP-S2	3.7	6.6	22	25	---

[a] σ_{01}: ground state absorption cross section; σ_{12}: first singlet excited state absorption cross section; σ_{34}: first triplet excited state absorption cross section; τ_{isc}: intersystem crossing time; τ_T: triplet state decay time. [b] All absorption cross sections were measured at 532 nm. [c] Data extracted from ref 27.

$$\frac{dn_{S_0}}{dt} = -W_{S_0 \rightarrow S_1} n_{S_0} + \frac{n_{S_1}}{\tau_{10}} \quad (4a)$$

$$\frac{dn_{S_1}}{dt} = W_{S_0 \rightarrow S_1} n_{S_0} - \frac{n_{S_1}}{\tau_{10}} - \frac{n_{S_1}}{\tau_{isc}} \quad (4b)$$

$$\frac{dn_{T_1}}{dt} = \frac{n_{S_1}}{\tau_{isc}} \quad (4c)$$

where $W_{S_0 \rightarrow S_1} = \sigma_{01} I/h\nu$, is the upward transition rate; h is the Planck constant; I is the irradiance of the laser with frequency ν. The relation between the fluorescence lifetime (τ_{fluo}), obtained from fluorescence decay experiment from S_1, and the first excited singlet state time (τ_{10}) and the intersystem crossing time is given by[36,37,44]

$$\frac{1}{\tau_{fluo}} = \frac{1}{\tau_{10}} + \frac{1}{\tau_{isc}} \quad (5)$$

where the relaxation from the first excited singlet state to the ground state includes contributions from radiative and internal conversion processes. Finally, the normalization condition for population fractions is $n_{S_0} + n_{S_1} + n_{T_1} = 1$, where n_i denotes the population fraction in its respective molecular state.

According to Beer's law, the equation that governs the irradiance variation, I, along the penetration depth, z, can be

dx.doi.org/10.1021/jp205963k | J. Phys. Chem. A 2012, 116, 18–26

written as[27,37,43,44]

$$\frac{dI}{dz} = -\alpha(t)I(t) \quad (6)$$

where the absorption coefficient, $\alpha(t)$, is given by[27,43,44]

$$\alpha(t) = N[n_{S_0}(t)\sigma_{01} + n_{S_1}(t)\sigma_{12} + n_{T_1}(t)\sigma_{34}] \quad (7)$$

The transmittance can be calculated by integrating Beer's law over the sample thickness. Since the detection system in the experiment measures the pulse fluence, we have also to carry out an integration over the full pulse duration. Such result is then normalized to the linearly transmitted energy.

The ground-state absorption cross-section, σ_{01}, can be obtained after determining the absorption and concentration of the solution according to $\sigma_{01} = 2.3A/NL$, where A is the absorbance measured at 532 nm, N is the concentration in molecules/cm^3, and L is the cuvette optical path (in cm). The values measured are shown at Table 4 for all molecules investigated.

To determine the effects of the ruthenium outlying groups on the absorption of singlet excited states, we performed Z-scan measurements at 532 nm using single 70 ps pulses. The use of single pulses allows the simplification of the rate equation analyses, since no appreciable population is formed in the triplet states, which reduces the system to the left of the Jablonski diagram. In addition, the S_1 relaxation can be neglected because the lifetime measured is much longer than the laser pulse duration (70 ps). It is important to mention that even the faster singlet decay time measured ($\approx$ 600 ps), for the compound H_2TPyP-S2, is almost 10 times longer than the single pulse employed. Figure 6a shows Z-scan transmittance for the H_2TPyP-S1 compound as a function of the 70 ps laser irradiance, measured when the sample is at the focal plane. Several Z-scan curves were obtained for different irradiances to guarantee that the transmittance was properly normalized. From them, the normalized transmittances at the focus, shown in Figure 6a, were determined. Since the triplet can be neglected, a numerical fitting shown by the solid line in Figure 6a was obtained by solving the eqs 4a−4c, with the triplet terms omitted. Since σ_{01} values were already obtained from the absorbance spectra, the only adjustable parameters needed to optimize the fitting is the S_1 absorption cross-section, σ_{12}. These values are shown in Table 4.

After determining the singlet state photophysical parameters σ_{01}, σ_{12}, and τ_{fluo}, with linear absorption, fluorescence decay, and single-pulse Z-scan experiments, we then proceeded to characterize the triplet state, for the purpose of evaluating the intersystem crossing time and the excited triplet state absorption cross-section. In order to obtain these values, we carried out Z-scan measurements, employing the complete pulse train. In this case, the complete five-energy-level diagram must be considered. With the same procedure used for the single-pulse experiment, the sample transmittance for each individual pulse in the train can be evaluated. When the normalized transmittance does not follow the pulse train profile, one may expect that the effect of a given pulse influences the subsequent pulses.

In Figure 6b, the solid squares show a typically normalized transmittance as a function of the number of pulses under the Q-switch envelope measured by the pulse train technique,[31] for the H_2TPyP-S1 sample placed at the focal plane.

These curves present saturation after the given number of pulses affecting the sample. Since the time delay between pulses is longer than the ground-state recovery time, the saturation indicates that the molecule is at a level different from the ground-state, and the only possibility is that it was promoted to the triplet state via the intersystem crossing. The normalized transmittance decrease, for different pulses in the train, indicates that σ_{01} is smaller than the excited state triplet absorption cross-section (σ_{34}).

In order to analyze the cumulative behavior observed for the pulse train using the already known singlet values, σ_{34} and τ_{isc} are needed as fitting parameters. While the first one is mainly responsible for the strength of the RSA process, the second one determines how fast the molecule moves to the triplet state. The fitting shown by the solid line is achieved by adjusting the experimental points to the complete five-energy-level diagram via the use of eqs 4a−4c and gives σ_{34} and τ_{isc}, which are also depicted in Table 4. Finally, laser flash photolysis measurements (not presented here) provide the triplet state decay time (τ_T), which is also shown in Table 4. This type of relaxation is also an intersystem crossing from the first triplet excited state to the singlet ground state. Here, an increase in the time taken by this kind of process is also observed. Unfortunately, both the triplet absorption cross-section spectrum and the quantum efficiency of the triplet formation were not measured because the samples presented a photodegradation process caused by the long exposure to the high fluence of the nanosecond pulses employed in the laser flash photolysis experiments.

The results summarized in Table 4 show that the presence of Ru(II) outlying groups causes an increase in the intersystem crossing time, which is deleterious for triplet population formation. This result is completely different from that observed when Ru(II) ion is inserted in the center of the macrocycle, as well as from the conclusions obtained in ref 25 for similar tetrapyridyl supramolecular systems. According to ref 25, an increase in the triplet formation quantum yield is expected due to the heavy atom effect. However, a careful analysis of this reference, as well as of other similar works,[15,26] shows that the authors do not measure the intersystem crossing time. Instead, they conclude that the porphyrin intersystem crossing is enhanced because of the absences of intersystem crossing from porphyrin ring to ruthenium moieties.

On the contrary, we directly measured, for the first time, the intersystem crossing time for such systems, showing its increase. Such observation implies that this mechanism can not be considered responsible for the observed fluorescence quenching. A possible explanation for the observed increase of the intersystem crossing time can be attributed to a distortion of the porphyrin ring due to outlying groups, which is deleterious to the spin−orbit coupling responsible for the intersystem crossing process.

4. CONCLUSION

In summary, we have synthesized two types of porphyrin structures and investigated the influence of the presence Ru(II) outlying moieties in the spectroscopic properties and excited-state dynamics of H_2TPyP. The results show that both absorbance and emission are affected by the presence of ruthenium groups, with the more significant influence being caused by the $[RuCl_2(PPh_3)CO]$ group. As for the absorbance spectrum, we observed that the Soret band is formed by three sub-bands associated with three different vibrational modes of the second excited singlet state. It was also observed that the presence of outlying moieties causes a noticeable enlargement in the Soret bandwidth, which is explained by the increase of the contribution of the sub-band with lower energy (called sub-band B_3).

Moreover, both Soret and Q bands suffer red shifts, indicating a decrease in the HOMO−LUMO gap. Furthermore, it is observed that the fluorescence signal is quenched considerably due to the presence of ruthenium groups, which is confirmed by the decrease of the emission quantum yield. The fluorescence decay time clearly supports the hypothesis that the quenching in the fluorescence signal is caused by the activation of new, faster, nonradiative decay paths. Concerning the excited-state dynamics, the most significant observation is related to the fact that the presence of outlying ruthenium groups causes a decrease of all intersystem crossing rates, probably caused by distortions of the porphyrin ring induced by the presence of the outlying groups. Such behavior is opposite that observed when Ru (II) ions are placed at the center of the macrocycle. Finally, the analysis of the complete set of experimental results shows that the fluorescence quenching observed can be attributed to two possible mechanisms: (i) energy transfer from porphyrin to outlying groups or (ii) creation of new vibrational modes due to the presence of ruthenium moieties.

AUTHOR INFORMATION

Corresponding Author

*Mailing address: Instituto de Física, Universidade Federal de Uberlândia, P.O. Box 359, 38400-902, Uberlândia, MG, Brazil. Fax: +55 (34) 3239-4106; e-mail: rns.sampaio@gmail.com.

ACKNOWLEDGMENT

The authors sincerely acknowledge the support provided by CNPq, INCT/INFo, CAPES, and FAPEMIG. R.N.S. is especially thankful to CAPES for the graduate scholarship. A.E.H.M. is particularly indebted to CNPq and CAPES for his research grants.

REFERENCES

(1) Kalyanasundaram, K. *Photochemistry of Polypyridine and Porphyrin Complexes*; Academic Press: San Diego, CA, 1992.

(2) Voet, D.; Voet, J. G. *Biochemistry*; John Wiley & Sons Inc.: New York, 1995.

(3) Mal'tsev, E. I.; Brusentseva, M. A.; Rumyantseva, V. D.; Lypenko, D. A.; Berendyaev, V. I.; Mironov, A. F.; Novikov, S. V.; Vannikov, A. V. *Polym. Sci. A* **2006**, *48*, 146–152.

(4) Konan, Y. N.; Gurny, R.; Allémann, E. *J. Photochem. Photobiol. B* **2002**, *66*, 89–106.

(5) Schmitt, F.; Govindaswamy, P.; Süss-Fink, G.; Ang, W. H.; Dyson, P. J.; Juillerat-Jeanneret, L.; Therrien, B. *J. Med. Chem.* **2008**, *51*, 1811–1816.

(6) Pavinatto, F. J.; Gameiro, A. F., Jr.; Hidalgo, A. A.; Dinelli, L. R.; Romualdo, L. L.; Batista, A. A.; Barbosa Neto, N. M; Ferreira, M.; Oliveira, O. N., Jr. *Appl. Surf. Sci.* **2008**, *245*, 5946–5952.

(7) Loppacher, C.; Guggisberg, M.; Pfeiffer, O.; Meyer, E.; Bammerlin, M.; Lüthi, R.; Schlittler, R.; Gimzewski, J. K.; Tang, H.; Joachim, C. *Phys. Rev. Lett.* **2003**, *90*, 066107.

(8) Mammana, A.; D'Urso, A.; Lauceri, R.; Purrello, R. *J. Am. Chem. Soc.* **2007**, *129*, 8062–8063.

(9) Lu, H.-P.; Mai, C.-L.; Tsia, C.-Y.; Hsu, S.-J.; Hsieh, C.-P.; Chiu, C.-L.; Yeh, C.-Y.; Diau, E. W.-G. *Phys. Chem. Chem. Phys.* **2009**, *11*, 10270–10274.

(10) Barbosa Neto, N. M.; De Boni, L.; Mendonça, C. R.; Misoguti, L.; Queiroz, S. L.; Dinelli, L. R.; Batista, A. A.; Zílio, S. C. *J. Phys. Chem. B* **2005**, *109*, 17340–17345.

(11) Barbosa Neto, N. M.; Oliveira, S. L.; Misoguti, L.; Mendonça, C. R.; Gonçalves, P. J.; Borissevitch, I. E.; Dinelli, L. R.; Romualdo, L. L.; Batista, A. A.; Zilio, S. C. *J. Appl. Phys.* **2006**, *99*, 123103.

(12) (a) Collini, E.; Ferrante, C.; Bozio, R. *J. Phys. Chem. B* **2005**, *109*, 2–5. (b) Fujiwara, K.; Monjushiro, H.; Watarai, H. *Chem. Phys. Lett.* **2004**, *394*, 349–353. (c) Gonçalves, P. J.; Barbosa Neto, N. M.; Parra, G. G; de Boni, L.; Aggarwal, L; Siqueira, J. P.; Misoguti, L.; Borissevitch, I. E.; Zílio, S. C. *Opt. Mater.* **2011**, DOI: 10.1016/j.optmat.2011.10.012.

(13) Sevian, A.; Ravikanth, M.; Kumar, G. R. *Chem. Phys. Lett.* **1996**, *263*, 241–246.

(14) Barbosa Neto, N. M.; Oliveira, S. L.; Guedes, I.; Dinelli, L. R.; Misoguti, L.; Mendonça, C. R.; Batista, A. A.; Zílio, S. C. *J. Braz. Chem. Soc.* **2006**, *17*, 1377–1382.

(15) Ghiroti, M.; Chiorboli, C.; Indelli, M. T.; Scandola, F.; Casanova, M.; Iengo, E.; Alessio, E. *Inorg. Chim. Acta* **2007**, *360*, 1121–1130.

(16) Basic, B.; McMurtrie, J. C.; Arnold, D. P. *Eur. J. Or. Chem.* **2010**, 4381–4392.

(17) Mayer, I.; Eberlin, M. N.; Tomazela, D. M.; Toma, H. E.; Araki, K. *J. Braz. Chem. Soc.* **2005**, *16*, 418–425.

(18) (a) Gonçalves, P. J.; Franzen, P. L.; Correa, D. S.; Almeida, L. M.; Takara, M.; Ito, A. S.; Zílio, S. C.; Borissevitch, I. E. *Spectrochim. Acta A* **2011**, *79*, 1532–1539. (b) Maximiano, R. V.; Piovesan, E.; Zilio, S. C.; Machado, A. E. H.; de Paula, R.; Cavaleiro, J. A. S.; Borissevitch, I. E.; Ito, A. S.; Gonçalves, P. J.; Barbosa Neto, N. M. *J. Photochem. Photobiol. A* **2010**, *214*, 115–120.

(19) Antipas, A.; Buchler, J. W.; Gouterman, M.; Smith, P. D. *J. Am. Chem. Soc.* **1978**, *100*, 3015–3024.

(20) Levine, L. M. A.; Holten, D. *J. Phys. Chem.* **1998**, *92*, 714–720.

(21) Tait, C. D.; Holten, D.; Barley, M. H.; Dolphin, D.; James, B. R. *J. Am. Chem. Soc.* **1985**, *107*, 1930–1934.

(22) Rodriguez, J.; Mcdowell, L.; Holten, D. *Chem. Phys. Lett.* **1998**, *147*, 235–240.

(23) Peters, J. W.; Pitts, J. N., Jr.; Rosenthal, J.; Fuhr, H. *J. Am. Chem. Soc.* **1972**, *94*, 4350–4351.

(24) Scandola, F.; Chiorboli, C.; Prodi, A.; Iengo, E.; Alessio, E. *Coord. Chemi. Rev.* **2006**, *250*, 1471–1496.

(25) Prodi, A.; Kleverlaan, C. J.; Indelli, M. T.; Scandola, F.; Alessio, E.; Iengo, E. *Inorg. Chem.* **2001**, *40*, 3498–3504.

(26) Casanova, M.; Zangrado, E.; Iengo, E.; Alessio, E.; Indelli, M. T.; Scandola, F.; Orlandi, M. *Inorg. Chem.* **2008**, *47*, 10407–10418.

(27) Barbosa Neto, N. M.; De Boni, L.; Rodrigues, J. J., Jr.; Misoguti, L.; Mendonça, C. R.; Dinelli, L. R.; Batista, A. A.; Zílio, S. C. *J. Porphyrins Phthalocyanines* **2003**, *7*, 452–456.

(28) Borissevitch, I. E. *J. Luminesc.* **1999**, *81*, 219–224.

(29) Sheik-Bahae, M.; Said, A. A.; Wei, T-H; Hagan, D. J.; Van Stryland, E. W. *IEEE J. Quantum Electron.* **1990**, *26*, 760–769.

(30) Sheik-Bahae, M.; Said, A. A.; Van Stryland, E. W. *Opt. Lett.* **1989**, *17*, 955–957.

(31) Misoguti, L.; Mendonça, C. R.; Zilio, S. C. *Appl. Phys. Lett.* **1999**, *74*, 1531–1533.

(32) Gonçalves, P. J.; De Boni, L.; Barbosa Neto, N. M.; Rodrigues, J. J., Jr.; Zílio, S. C.; Borissevitch, I. E. *Chem. Phys. Lett.* **2005**, *407*, 236–241.

(33) Qian, D.-J.; Planner, A.; Miyake, J.; Frackowiak, D. J. *Photochem. Photobiol. A* **2001**, *144*, 93–99.

(34) Dinelli, L. R.; Von Poelhsitz, G.; Castellano, E. E.; Ellena, J.; Galembeck, S. E.; Batista, A. A. *Inor. Chem.* **2009**, *48*, 4692–4700.

(35) Spellane, P. J.; Gouterman, M.; Antipas, A.; Kim, S.; Liu, Y. C. *Inorg. Chem.* **1980**, *19*, 386–391.

(36) Lakowicz, J. R. *Pricinples of Fluorescence Spectroscopy*; Kluwer Academic/Plenum Publishers: New York, 1999.

(37) Valeur, B. *Molecular Fluorescence: Principles and Applications*; Wiley-VHC: New York, 2002.

(38) Kalyanasundaram, K. *Inorg. Chem.* **1984**, *23*, 2453–2459.

(39) Eaton, D. F. *Pure Appl. Chem.* **1988**, *60*, 1107–1114.

(40) Mendonça, C. R.; dos Santos, D. S.; De Boni, L.; Balogh, D. T.; Oliveira, O. N., Jr.; Zílio, S. C. *Adv. Mater.* **2000**, *12*, 1126–1129.

(41) Franzen, P. L.; De Boni, L.; dos Santos, D. S.; Mendonça, C. R.; Zílio, S. C. *J. Phys. Chem. B* **2004**, *108*, 19180–19183.
(42) Klessinger, M.; Michl, J. *Excited States and Photochemistry of Organic Molecules*; VCH Publishers Inc.: New York, 1995.
(43) Mendonça, C. R.; Gaffo, L.; Misoguti, L.; Moreira, W. C.; Oliveira, O. N., Jr.; Zílio, S. C. *Chem. Phys. Lett.* **2000**, *323*, 300–304.
(44) Gonçalves, P. J.; Borissevitch, I. E.; Zilio, S. C. *Chem. Phys. Lett.* **2009**, *469*, 270–273.